UC SANTA BARBARA
engineering

Igor Mezic,
Mechanical Engineering,
UC Santa Barbara

# *Report on ONR-MURI Work in 2011*

The convergence of research and innovation.

# Introduction

-Ergodic-theory based methods for coherent structure identification in 3D+1 flows.

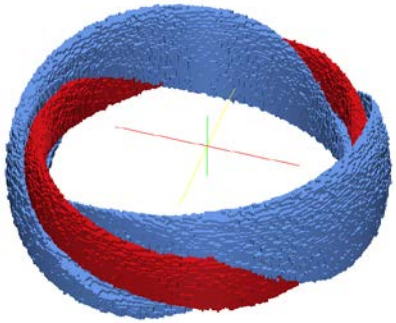

-Mesohyperbolicity and reaction dynamics at 1000 meter depth Gulf of Mexico model.

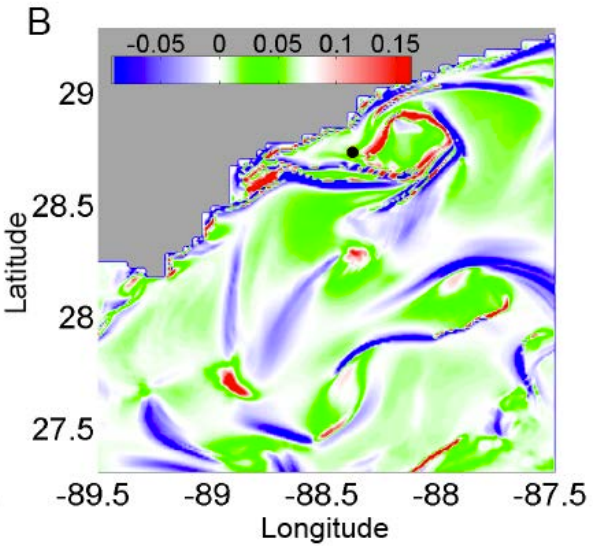


-An experimental testbed for Lagrangian dynamics in convective flows.

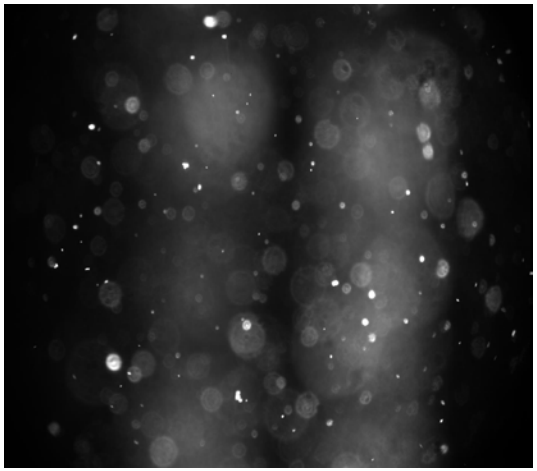

# Coherent Structures using Ergodic Theory

## Measure-preserving, discrete dynamics:

$$x_{i+1} = T(x_i),$$
$$y_i = f(x_i),$$

$$i \in \mathbb{Z},\ x_i \in M,\ T : M \to M,$$
$$\mu(T^{-1}A) = \mu(A)$$

We call the function $f^*$ the time average of a function $f$ under $T$ if

$$f^*(x) = \lim_{n\to\infty} \frac{1}{n} \sum_{i=0}^{n-1} f(T^i x)$$

*Time averages* and *invariant measures*:

$$f^*(x) = \int_M f \, d\mu_x$$

Partition of M into level sets of $f^*$ is denoted $\zeta_f$

# Visualization

Define the Koopman operator : $U : L^1 \to L^1$, by

$$Uf(x) = f \circ T(x),$$

$f^*$ is constant on orbits i.e.

$$Uf^*(x) = f^*(x).$$

The operator

$$P_T(f) = f^*$$

can be considered as a member of a family of operators $P_T^\omega$,

$$P_T^\omega(f) = f_\omega^* = \lim_{n\to\infty} \frac{1}{n} \sum_{j=0}^{n-1} e^{i2\pi j\omega} f(T^j(x)),$$

# Visualization

## Ergodic partition constructively:

**Lemma 1** *Let $M$ be a compact metric space and $T : M \to M$ a $C^r, r \geqslant 1$, diffeomorphism . Assume there exist a complete system of functions $\{f_i\}, f_i \in C(M)$, i.e. finite linear combinations of $f_i$ are dense in $C(M)$. The ergodic partition of a $C^r, r \geqslant 1$ diffeomorphism $T : M \to M$ on $M$ is*

$$\zeta_e = \bigvee_{i \in \mathbb{N}} \zeta_{f_i}.$$

$$\begin{aligned} x' &= x + y + \varepsilon \sin(2\pi x) \quad [mod\ 1] \\ y' &= y + \varepsilon \sin(2\pi x) \quad [mod\ 1] \end{aligned}$$

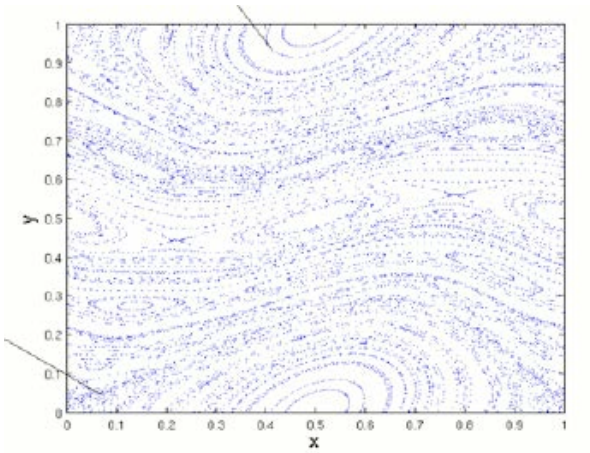


$$f_1 = \cos(2\pi y)$$
$$f_2 = \cos(2\pi x)\cos(2\pi y)$$
$$f_3 = \sin(4\pi x)\sin(4\pi y)$$
$$f_4 = \sin(10\pi x)\sin(10\pi y)$$

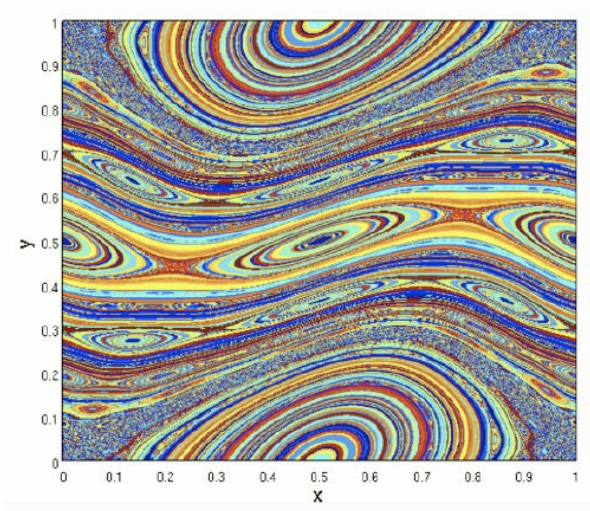

# Ergodic Quotient

$$x \xrightarrow{\Phi} \mu_x$$

$$\frac{1}{N}\sum_{n=0}^{N-1} f \circ T^n(x) \xrightarrow[N\to\infty]{\text{weak-}*} \int f d\mu_x$$

Each initial condition has an ergodic empirical measure associated to it.

$$\tilde{f}(x) = \frac{1}{N}\sum_{n=0}^{N-1} f \circ T^n(x)$$

By averaging a basis of continuous functions on the state space manifold, we can represent empirical measures in a weak sense.

$$f_k(x) = e^{i2\pi(k\cdot x)}, \quad k \in \mathbb{Z}^d$$

$$x \xrightarrow{\Phi} [\ldots, \tilde{f}_k(x), \ldots] \subset l_\infty(\mathbb{Z}^d)$$

We obtain representation of ergodic measures in a sequence space.

**Theorem. (Discrete topology)** Ergodic quotient map separates the ergodic partition, i.e., points $x$ and $y$ are in the same ergodic set iff

$$\Phi(x) = \Phi(y)$$

Ergodic partition is equivalent to the quotient of the state space by level sets of all time-averaged functions

# Metric Geometry

**Ergodic Quotient**

$$\xi = \{\Phi(x) : x \in \mathcal{M}\} \subset l_\infty$$

$$\|\mu_x - \mu_y\|^2 = \sum_{k \in \mathbb{Z}^d} \frac{\left|\tilde{f}(x) - \tilde{f}(y)\right|^2}{[1 + (2\pi \|k\|)_2]^s}$$

Endow the ambient space with a weighted Euclidean metric that corresponds to negative-index Sobolev space of containing invariant measures.

**What can geometry of the ergodic quotient tell us about corresponding state space structures?**

State space

Ergodic Quotient

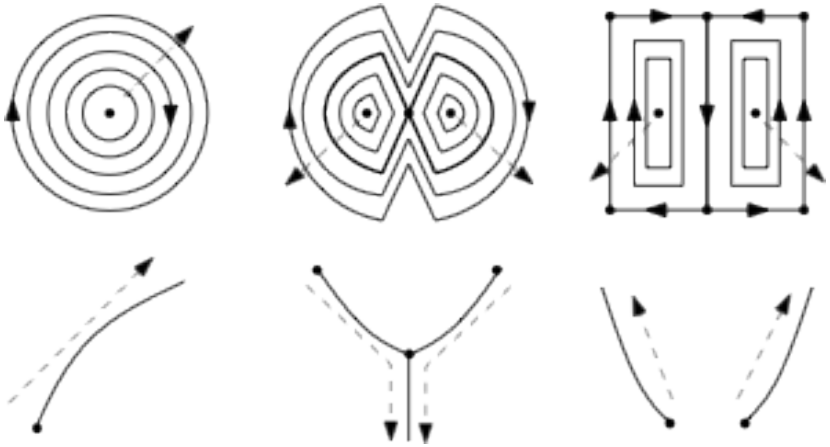

Sufficiently many local integrals of motion imply local continuity of the ergodic quotient.

# Computational Geometric Analysis

**Goal: detect locally connected subsets of EQ to identify trajectories that lie within a regions with local integrals of motion.**

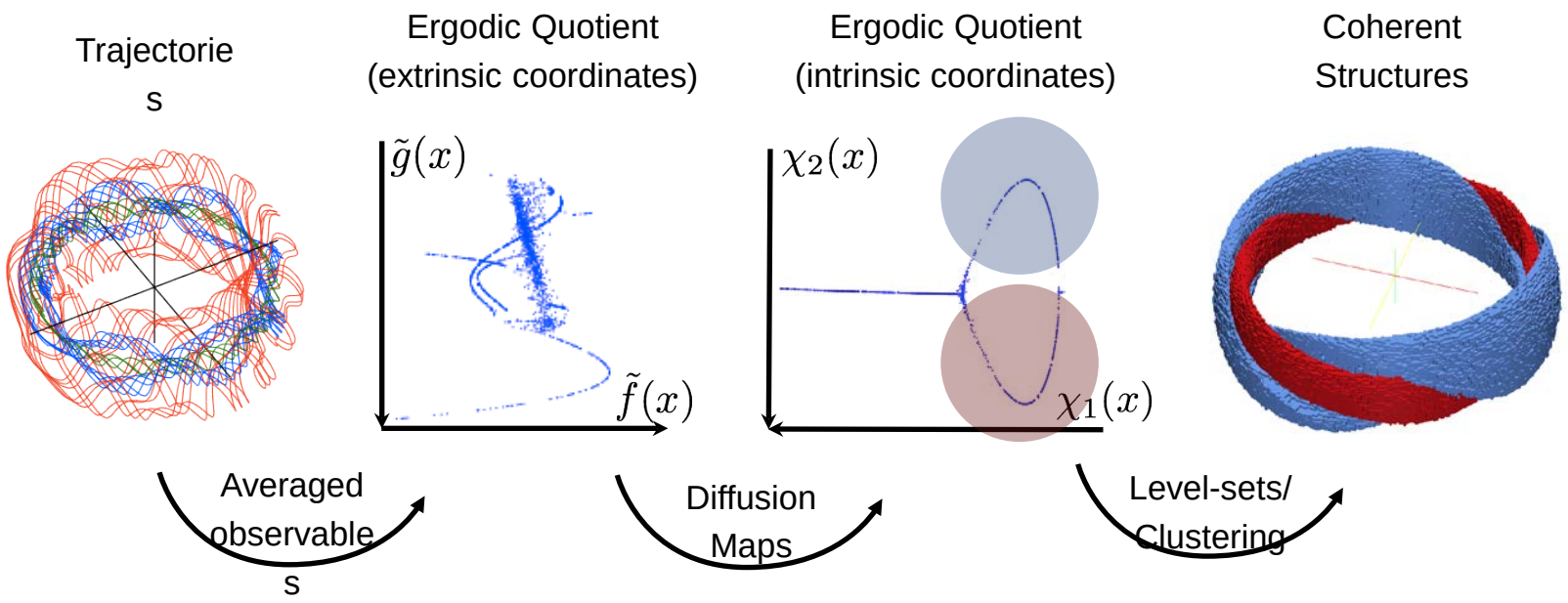


Compute numerical diffusion modes on the ergodic quotient to obtain low-dimensional representation of the ergodic quotient.

Geometric clustering, e.g., *k*-means, in diffusion space can then extract connected subsets. Color trajectories based on the membership in clusters.

# ABC Flow

## ABC flow: Global Structure

$$\begin{bmatrix}\dot{x}\\ \dot{y}\\ \dot{z}\end{bmatrix} = \begin{bmatrix}A\sin z + C\cos y\\ B\sin x + A\cos z\\ C\sin y + B\cos x\end{bmatrix} \qquad A=\sqrt{3}, B=\sqrt{2}, C=1$$

### State space clusters

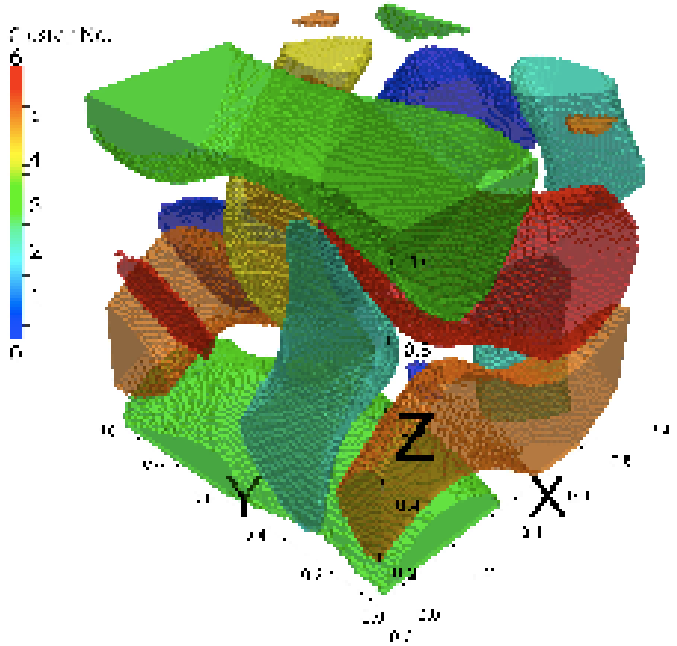


(a) Six subsets in the state space corresponding to six clusters of aggregation. Subsets contain primary vortices of the ABC flow. The chaotic sea between vortices is the seventh cluster and appears as the void between vortices.

### Ergodic Quotient

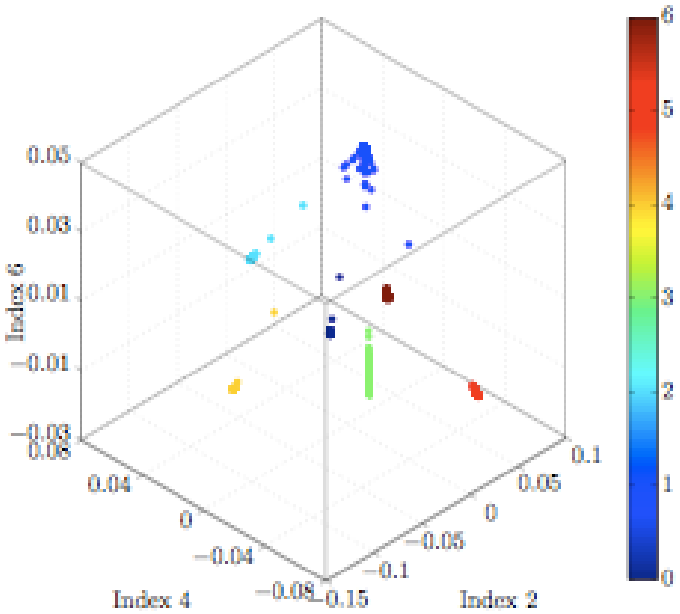


(b) Projection of ergodic quotient onto three out of ten diffusion coordinates used for clustering. Points were colored according to membership in clusters. The central cluster corresponds to the chaotic sea.

FIG. 2: Six primary vortices extracted by k-means clustering ($k = 7$) of projection of ergodic quotient onto first 10 diffusion coordinate. ABC flow (10) was simulated with $A = \sqrt{3}$, $B = \sqrt{2}$, $C = 1$, from $N = 1000$ initial conditions uniformly distributed in basic periodicity cell $[0, 1)^3$, with observables cut off at wavenumber $K = 10$, and convergence tolerance ATOL $= 2 \times 10^{-4}$.

# ABC Flow: Comparison

**Theory:**

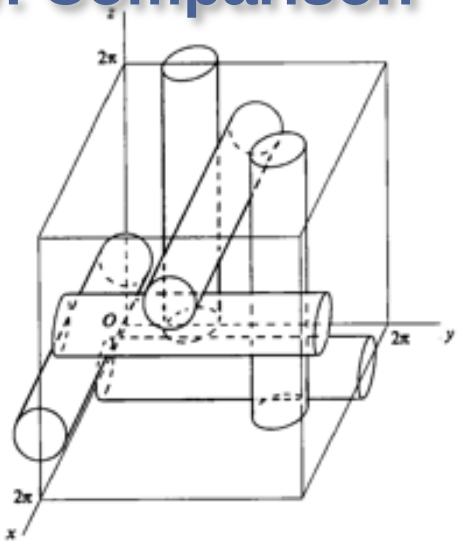


[Dombre et al.,1986]

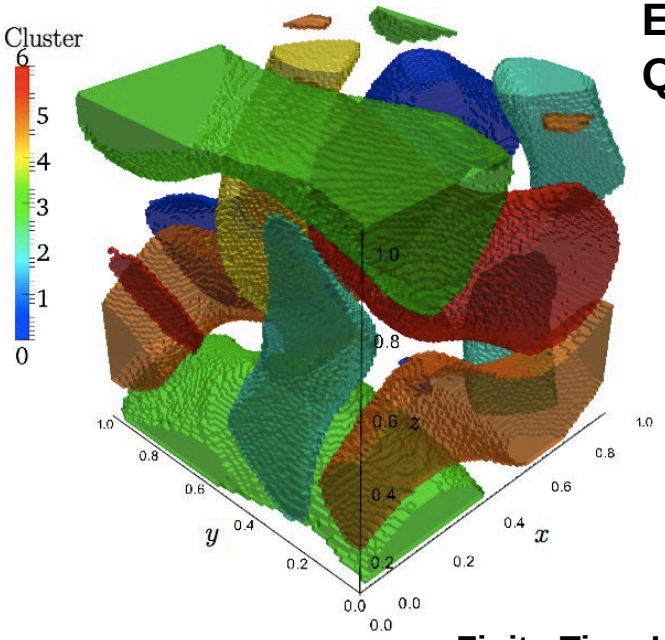


**Ergodic Quotient**

**Finite-Time Lyapunov Exp.**

**Ulam's Method**

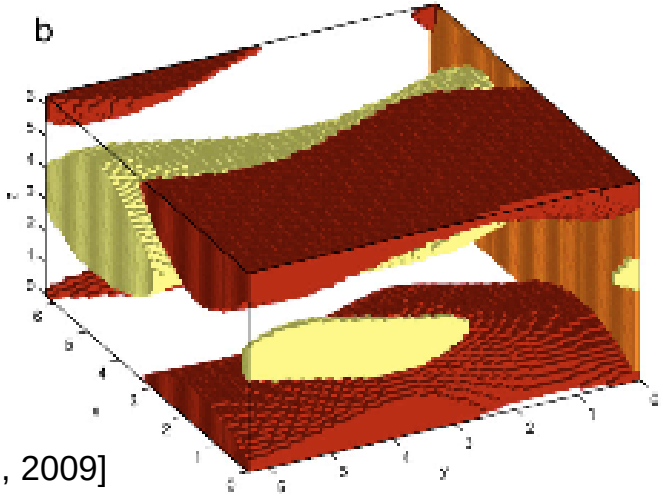


[Froyland, Padberg, 2009]

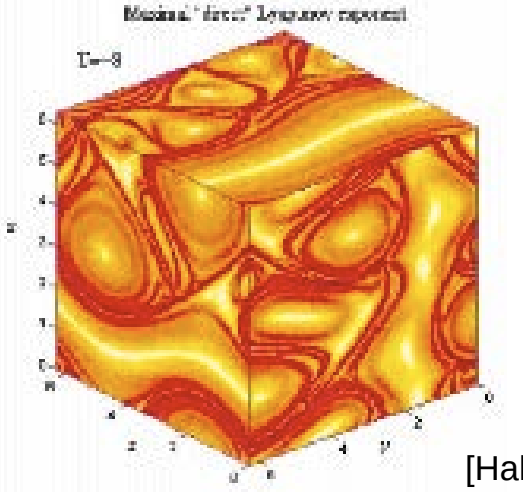


[Haller, 2001]

# ABC flow: Primary vortex

Ergodic Quotient

State space colored by a single diffusion mode

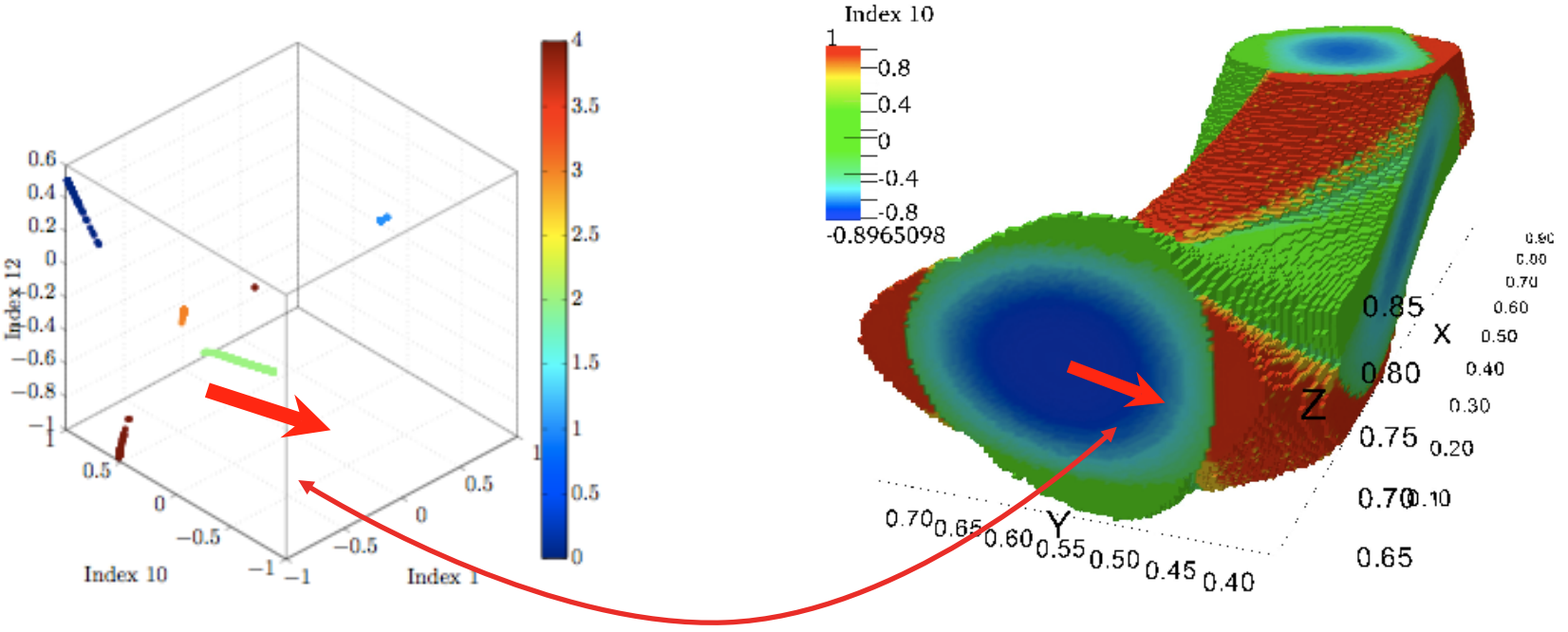


FIG. 3: A primary vortex aligned with the $x$-axis of the ABC flow ($A = \sqrt{3}$, $B = \sqrt{2}$, $C = 1$). Results are based on $N = 500$ trajectories initialized uniformly on the $\{0\} \times [0.35, 0.8] \times [0.6, 0.9]$ plane, with observables cut off at wavenumber $K = 10$, and convergence tolerance $\mathrm{ATOL} = 2 \times 10^{-4}$.

The diffusion coordinate that varies monotonically along continuous segments of ergodic quotient correctly parametrizes layers in an elliptic region.

# Kinematic, 3D+time flow

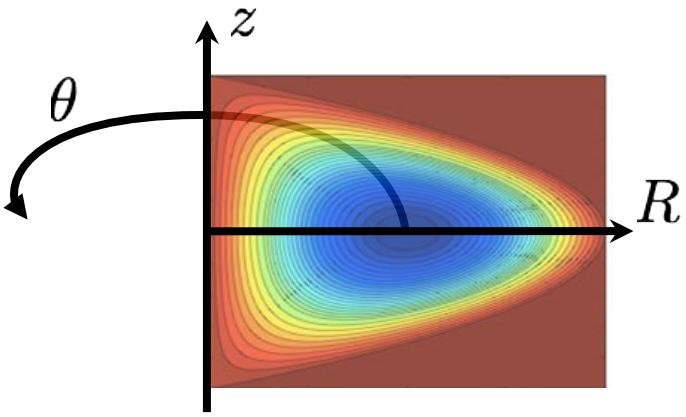


Hill's Vortex

Perturbation

$$\begin{bmatrix} \dot{R} \\ \dot{z} \\ \dot{\theta} \end{bmatrix} = \begin{bmatrix} 2Rz \\ 1 - 4R - z^2 \\ \frac{c}{2R} \end{bmatrix} + \varepsilon \begin{bmatrix} \sqrt{2R}\sin\theta \\ \frac{z}{\sqrt{2R}}\sin\theta \\ 2\cos\theta \end{bmatrix} \sin 2\pi t$$

Swirl

$(R, z, \theta) \in \mathbb{R}^+ \times \mathbb{R} \times \mathbb{T}$

- Unperturbed: Hamiltonian at each slice $\theta = const.$
- Volume preserving swirl and perturbation
- KAM behavior at small $c = \varepsilon$

## Invariant sets (using EQ)

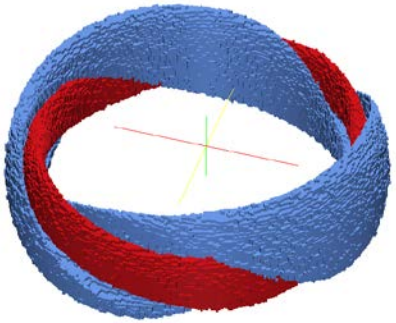

Canonical coordinates

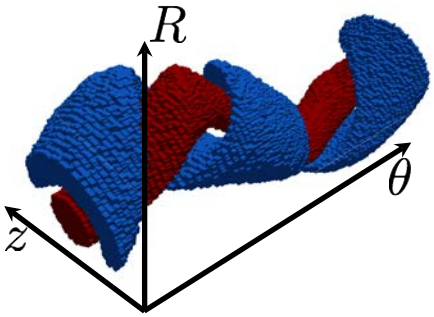


Angle unraveled

Two elliptic regions exist.

- Red, leftover from unperturbed elliptic region;
- Blue, borne out of separatrix for unperturbed case.

# Bifurcation uncovered using ergodic quotient

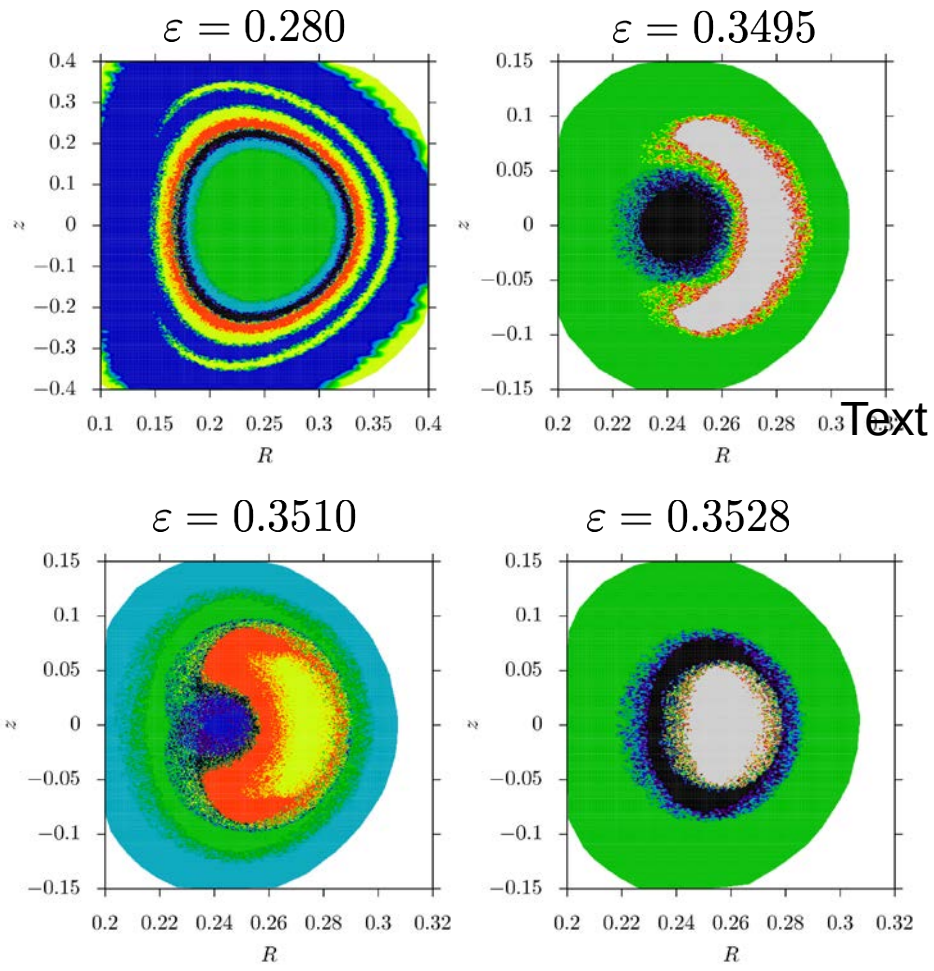


Text

## Conclusions:

- **Ergodic quotient is useful** for discovering unknown features
- **New bifurcation uncovered**, Consistent with a saddle-node collision mechanism for periodic sets
- Similar phenomenon seen in 1:2 resonances for Hamiltonian systems, e.g., spring-pendulum oscillator [Broer ’03]

# Mesohyperbolicity

**Notation:**

- $\phi_{t_0}^{t+T}(\mathbf{x}_0)$ : the map of $A$ mapping the fluid particle starting at time $t_0$ at point $\mathbf{x}_0 \in \mathbb{R}$ to its position $\mathbf{x}$ at time $t_0 + T$.
- $D\phi_{t_0}^{t+T}(\mathbf{x}_0)$ is the Jacobian matrix $J(\mathbf{x}_0) = \partial\mathbf{x}/\partial\mathbf{x}_0$.

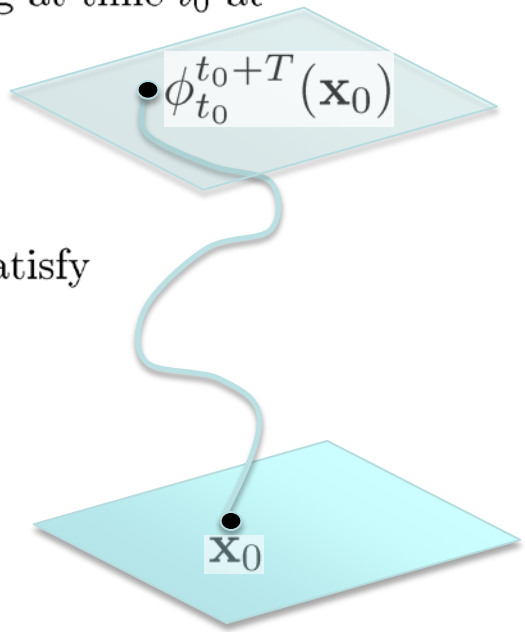


**Note:**

$\mathbf{v}$ is volume-preserving so the eigenvalues $\lambda_{1,2}(\mathbf{x}_0)$ of $J(\mathbf{x}_0)$ satisfy

$$\det(J(\mathbf{x}_0)) = \lambda_1(\mathbf{x}_0)\lambda_2(\mathbf{x}_0) = 1.$$

Thus, they are either real and

$$\lambda_1(\mathbf{x}_0) = 1/\lambda_2(\mathbf{x}_0)$$

or complex conjugate on the unit circle,

$$|\lambda_{1,2}(\mathbf{x}_0)| = 1.$$

A trajectory starting at $\mathbf{x}_0$ is

*mesohyperbolic* if $\lambda_{1,2}(\mathbf{x}_0)$ are real and

*mesoelliptic* if the eigenvalues are complex conjugate.

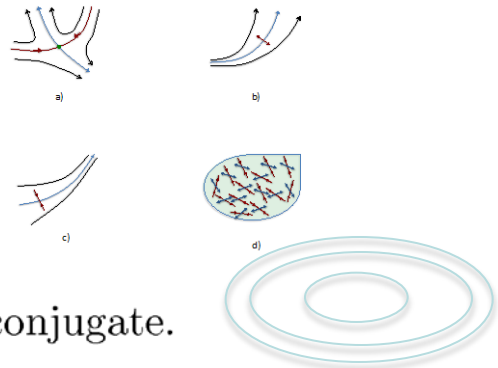

# Mesohyperbolicity in 2D

**Theorem** A trajectory is mesohyperbolic on interval $[t_0, t_0 + T]$ provided

$$(T^2 \det \nabla \mathbf{v}^*(\mathbf{x}_0, t_0, T) - 4) \det \nabla \mathbf{v}^*(\mathbf{x}_0, t_0, T) > 0$$

and mesoelliptic if

$$(T^2 \det \nabla \mathbf{v}^*(\mathbf{x}_0, t_0, T) - 4) \det \nabla \mathbf{v}^*(\mathbf{x}_0, t_0, T) < 0$$

.

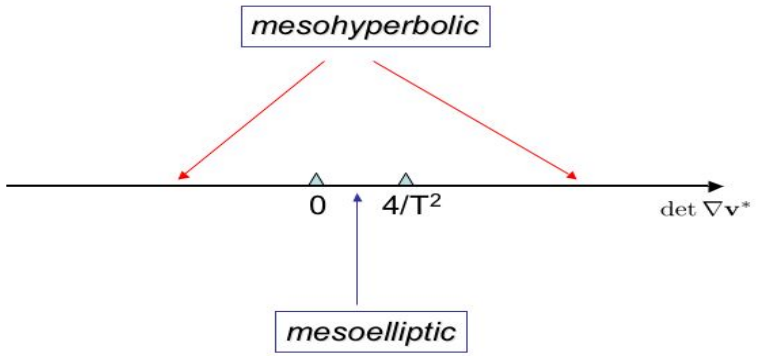

# Gulf Oil Spill Prediction

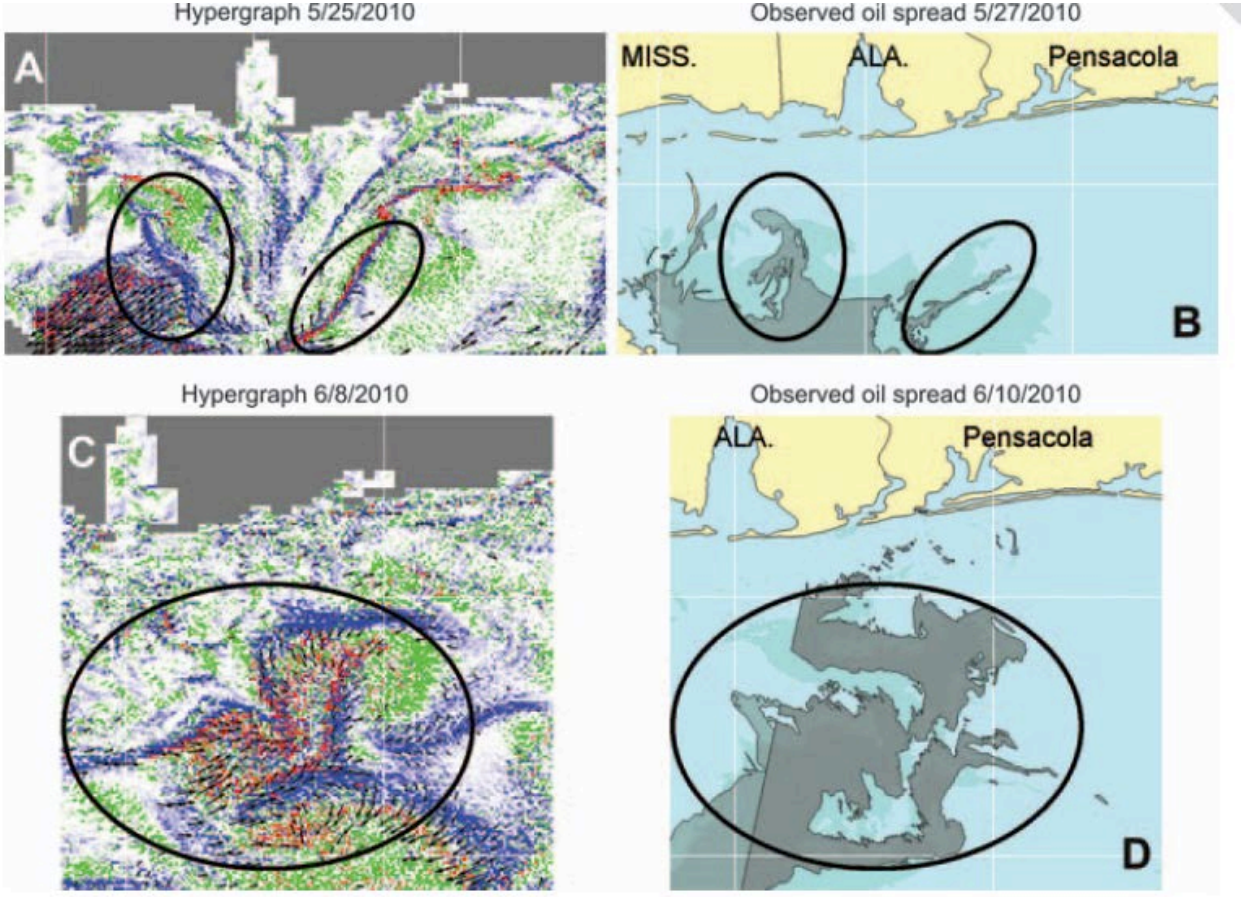


**Fig. 3.** (**A**) Ocean hypergraph map in front of the Biloxi-Pensacola shoreline on 25 May, forecasting strong oil incursion toward the coastline (circled) in the following 3 days. (**B**) NOAA's oil spread estimate in front of the Biloxi-Pensacola shoreline on 27 May. The major directions of oil spread were predicted by the hypergraph map 2 days earlier. The oil reached the shore several days later, on 2 June. (**C**) Ocean hypergraph map in front of Pensacola on 8 June, forecasting a strong oil mixing event in front of the shoreline and extension of the oil slick toward Panama City Beach in the following 3 days. (**D**) NOAA's oil spread estimate on 10 June in front of Pensacola. The oil developed a large slick forecasted by the hypergraph map 2 days earlier and continued to flow toward Panama City Beach.

*Analysis based on*

$$\det \nabla \mathbf{v}^*(\mathbf{x}_0)$$

*In 2-D AND 3-D*

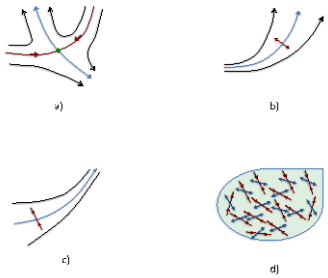

Robust, hyperbolic behavior

*I.M., S. Loire, V. Fonoberov, P. Hogan,* ***Science*** *(2011)*

# Deep Water Bacterial Population

- Model: the HYbrid Coordinate Ocean Model (HYCOM) hydrodynamic model

  +

  mass action chemical reaction model

  +

  backward-forward Lagrangian particle evolution.
- Primary and secondary hydrocarbon consumers
- Primary: 1/3 biomass+1/3 CO2 + 1/3 secondary chemical compound
- Secondary: ½ biomass +1/2 cO2

*With D. Valentine, S. Ilic, S. Loire, P. Hogan et al (PNAS)*

# Autoinnoculation

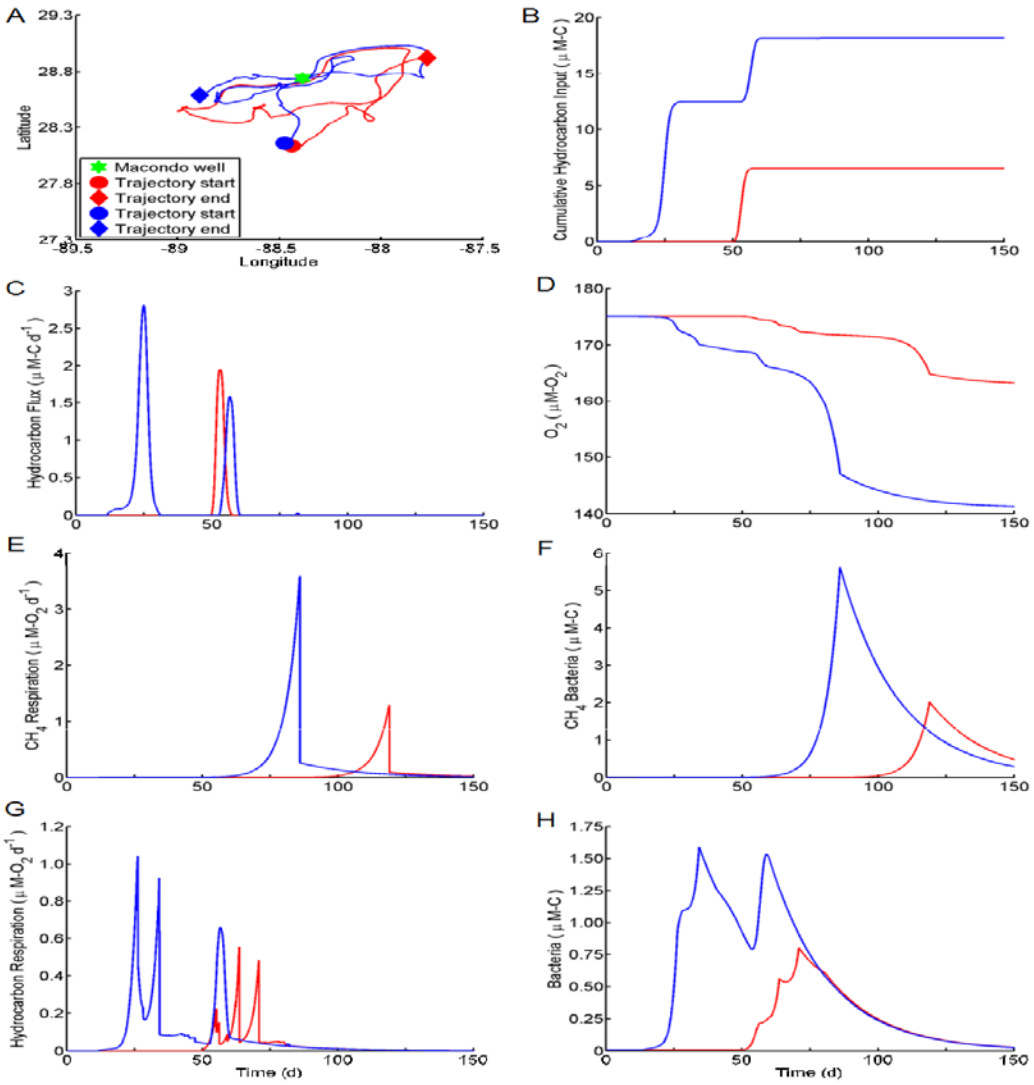

# Autoinnoculation

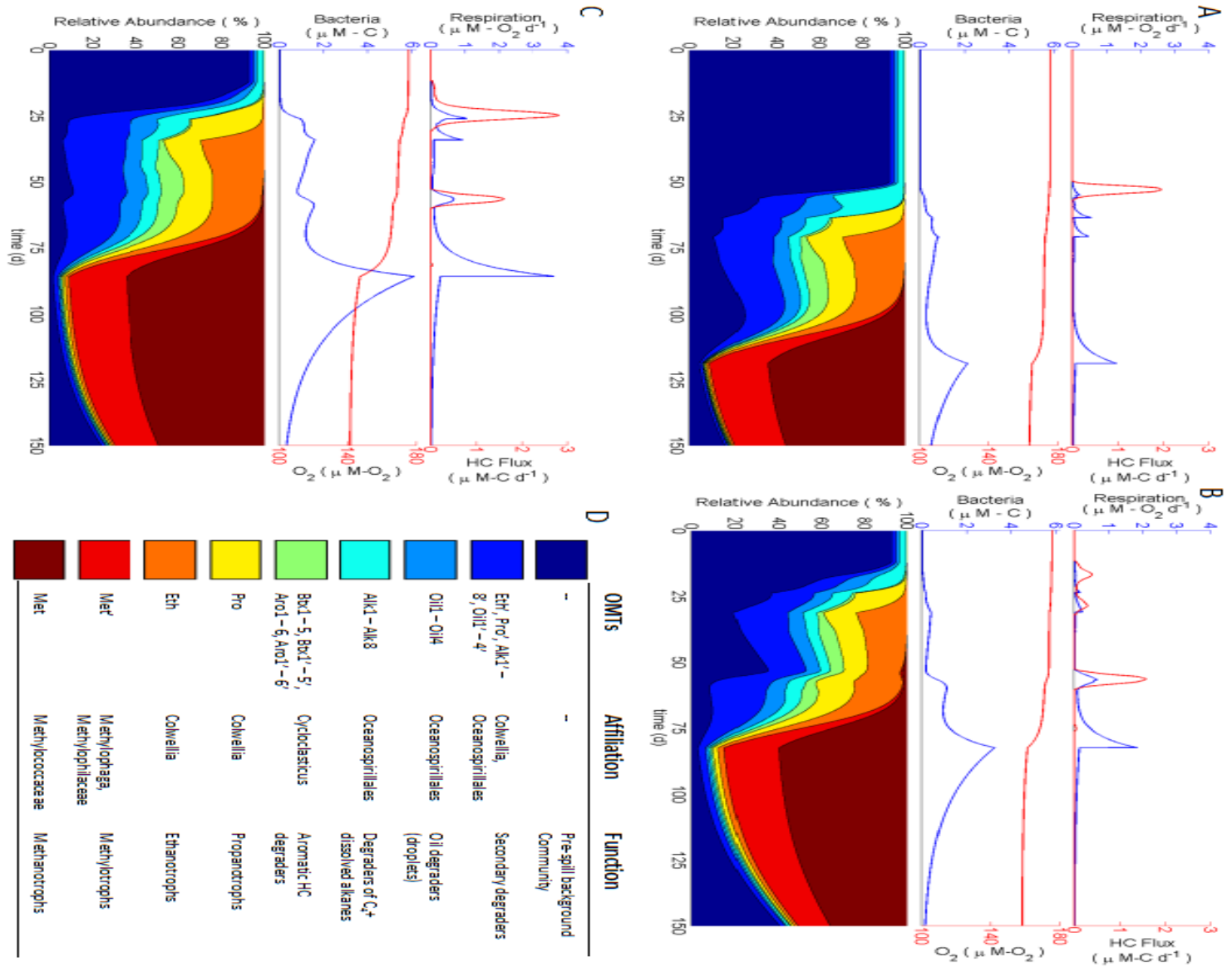

# Mesohyperbolicity

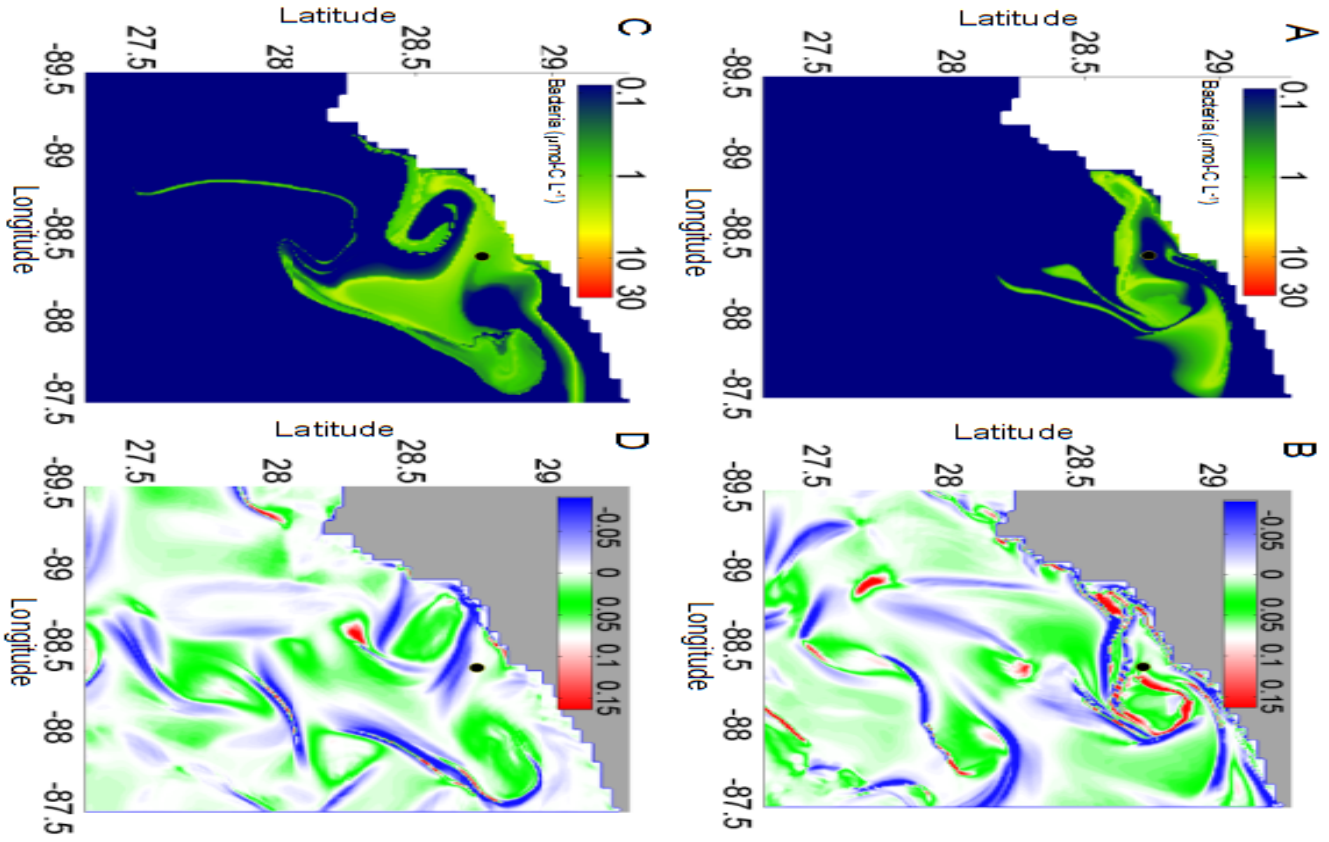

# Model vs Data

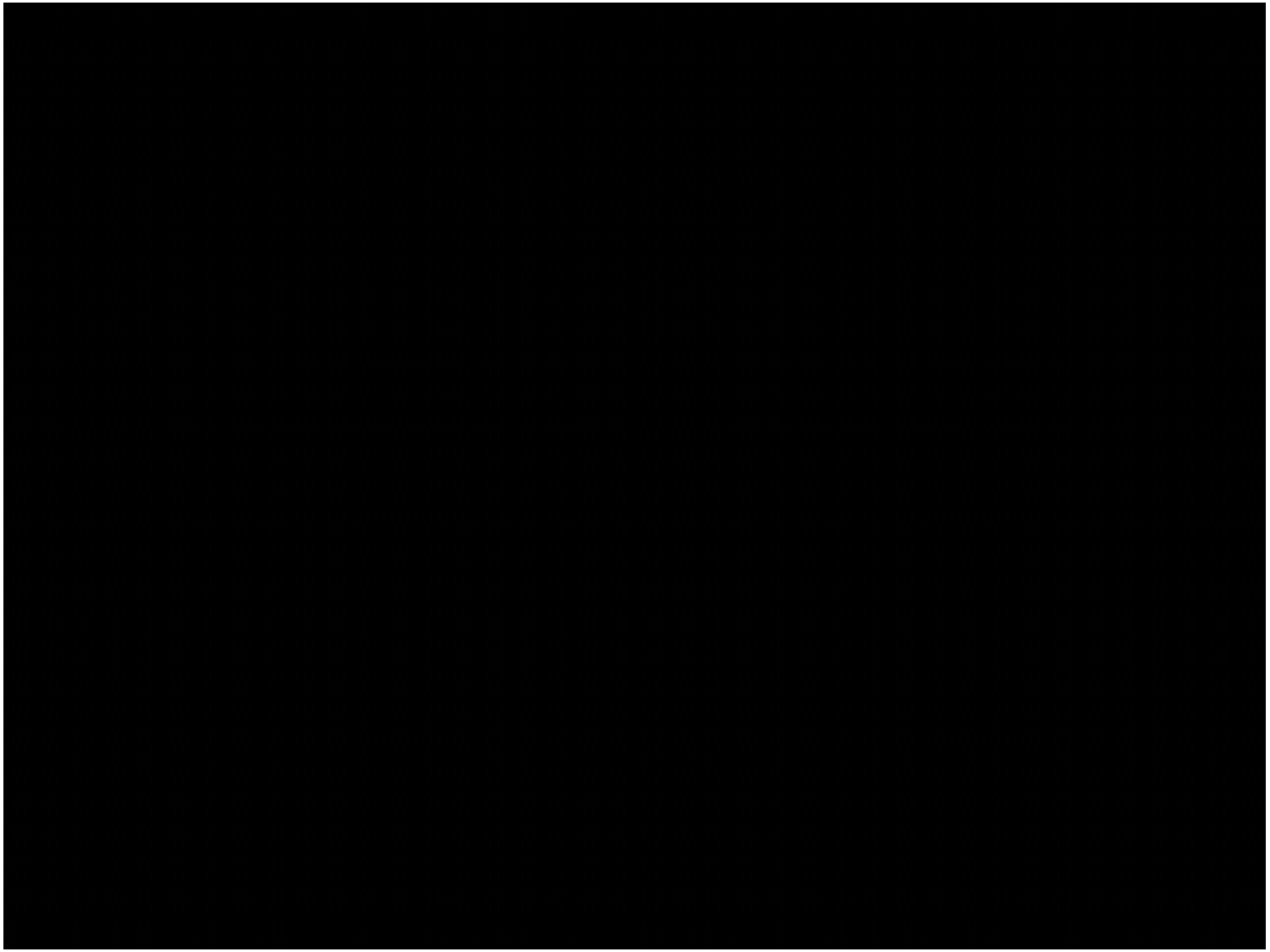

*Observations by Kessler et al, Camilli, et al, Diercks et al, Joye et al, Valentine et al, Hazen et al.*

# Mesohyperbolicity in 3D

Classification of Mesohyperbolicity). A mesohyperbolic solution $\varphi(T, t_0, x)$ is of one of the following types:

(i) $\mu_1, \mu_2, \mu_3 \in \mathbb{R}$ with $|\mu_1| \leq |\mu_2| < 1 < |\mu_3|$, which is equivalent to

$$\Delta > 0, \quad R(\frac{8}{T^2} - 2Q - 3TR) < 0.$$

(ii) $\mu_1, \mu_2, \mu_3 \in \mathbb{R}$ with $|\mu_1| < 1 < |\mu_2| \leq |\mu_3|$, which is equivalent to

$$\Delta > 0, \quad R(\frac{8}{T^2} - 2Q - 3TR) > 0.$$

(iii) $\mu_1, \mu_2 \in \mathbb{C}, \mu_3 \in \mathbb{R}$ with $|\mu_1| = |\mu_2| < 1 < |\mu_3|$, which is equivalent to

$$\Delta < 0, \quad R > 0.$$

(iv) $\mu_1 \in \mathbb{R}, \mu_2, \mu_3 \in \mathbb{C}$ with $|\mu_1| < 1 < |\mu_2| = |\mu_3|$, which is equivalent to

$$\Delta < 0, \quad R < 0.$$

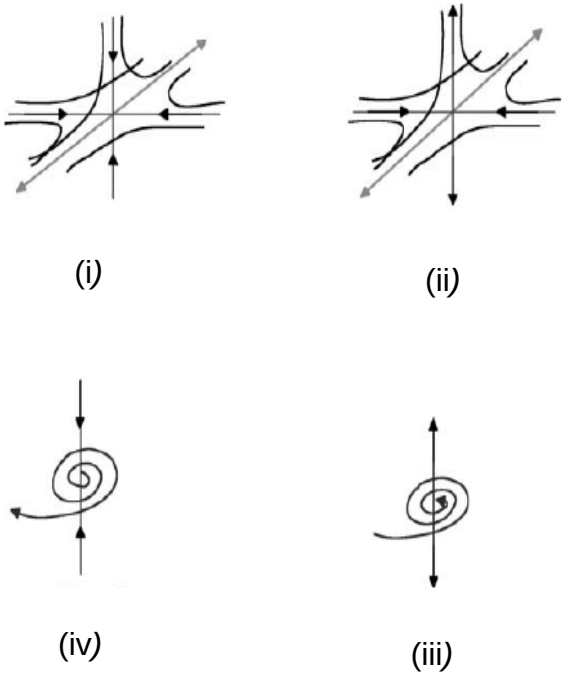


where $\triangle$ is a function of final time $T$, and matrix invariants $R, Q$.

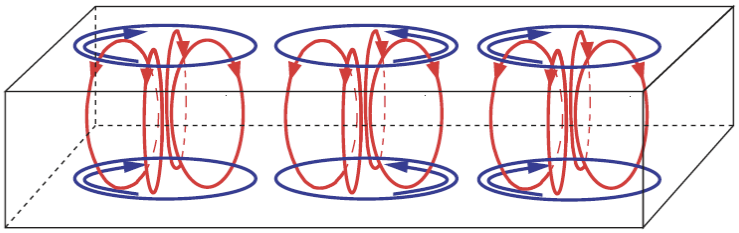

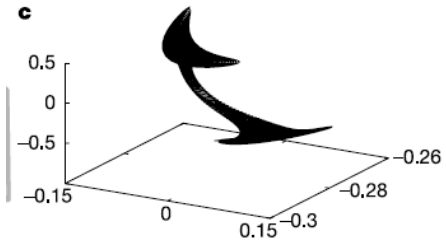


*With S. Siegmund (Dresden), M Budisic.*

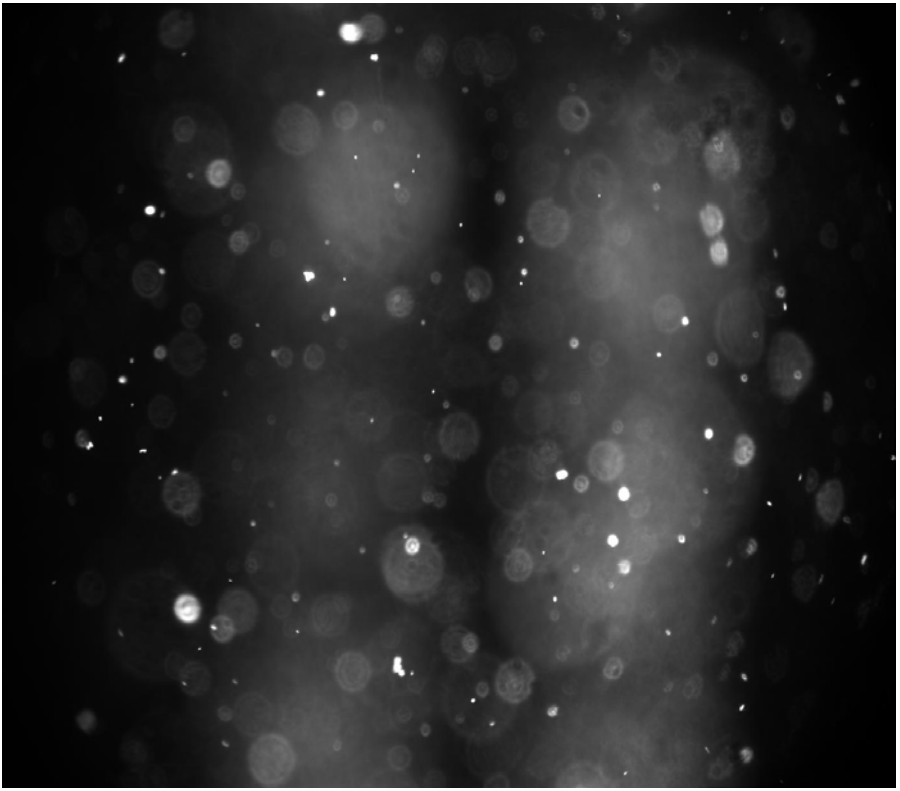

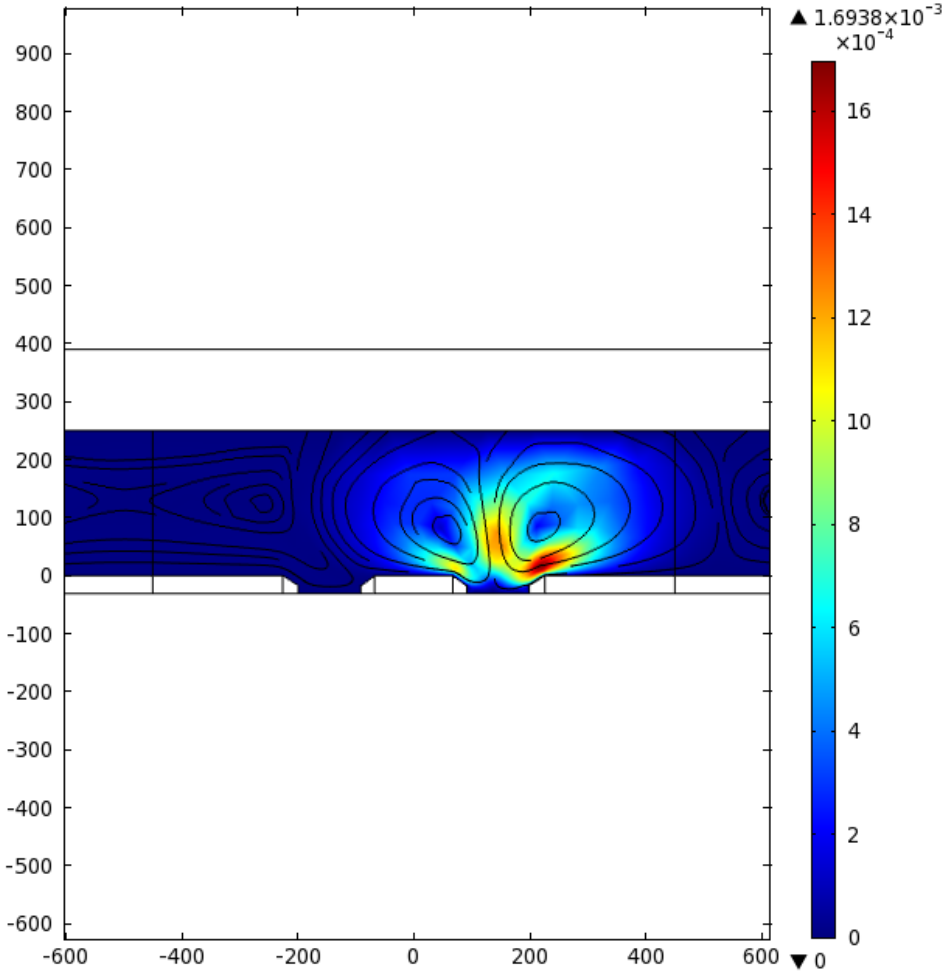
▲ 1.6938×10^-3
×10^-4
16
14
12
10
8
6
4
2
0
▼ 0
900
800
700
600
500
400
300
200
100
0
-100
-200
-300
-400
-500
-600
-600
-400
-200
0
200
400
600

# Conclusions

-Development of ergodic partition theory for 3D+1 leads to discovery of new bifurcations without use of Poincare maps.

-Methods applied to study of evolution of bacterial population during to gulf oil spill –

- The puzzle of missing oil resolved.
- Substantial predictive skill.
- Close correlation of mesohyperbolic regions with high reaction activity discovered.
- Of interest for future validation of Lagrangian methods.
- Ongoing succesfull collaboration with NRL (P. Hogan)
- Coverage in NYTimes, Wall Steet Journal, USA Today, Scientific American…

-3D+1 Mesohyperbolicity theory developed.

-Experimental testbed developed enabling visualization and extraction of Lagrangian features of 3D+1 flows.

Papers: D. Valentine, I. Mezic et al., “Dynamic autoinoculation and the microbial ecology of a deep water hydrocarbon irruption”, PNAS 109, (2012)

M. Budisic and I. Mezic “Geometry of the ergodic quotient reveals coherent structures in flows”, Submitted to Physica D (2012).

P. Kauffmann, S. Loire and I. Mezic. “A Theoretical and Experimental Study of Electrothermal Flows” Submitted to Journal of Physics D- Applied Physics.

S. Loire and I. Mezic, “Spatial Filter Averaging Approach of Probabilistic Method to Linear Second-Order Partial Differential Equations of the Parabolic Type”, Submitted to J. Computational Physics